



Case report

FDG-PET and CT findings of activated brown adipose tissue in a patient with paraganglioma

Yuko Ogawa^a, Koichiro Abe^{a,*}, Akiko Sakoda^b, Hiromi Onizuka^c, Shuji Sakai^a^a Departments of Diagnostic Imaging and Nuclear Medicine, Tokyo Women's Medical University, Tokyo, Japan^b Departments of Urology and Pathology, Tokyo Women's Medical University, Tokyo, Japan^c Departments of Pathology, Tokyo Women's Medical University, Tokyo, Japan

ARTICLE INFO

Keywords:

Brown adipose tissue
BAT
Paraganglioma
FDG-PET/CT
Contrast-enhanced CT

ABSTRACT

A 17-year-old female had been complaining of a headache for 6 years. She presented severe hypertension (200/138 mmHg) on admission. CT showed a hypervascular tumor behind the urinary bladder and a swelling of the right internal obturator node. Intense FDG uptakes were identified in the both lesions. High FDG accumulation was also observed in the brown adipose tissue (BAT) throughout the patient's body, and intense contrast enhancement was found in the BAT on CT. The diagnosis was a malignant paraganglioma with obturator node metastasis. The post-surgery FDG-PET/CT examination revealed that the FDG accumulations in the BAT had completely disappeared.

1. Introduction

F-18 fluorodeoxyglucose (FDG) positron emission tomography/computed tomography (PET/CT) has been used in many clinical settings to deal with malignant tumors, and it has become an indispensable imaging tool for managing patients with malignant tumors. Although FDG intrinsically accumulates in many types of malignant tissues, physiological FDG uptakes — including those in brown adipose tissue (BAT) — have also been widely recognized, and the physiological FDG uptakes might lead to false-positive results.

BAT is present primarily in infants and young children, but healthy adults also possess significant deposits of BAT [1,2]. BAT plays an important role in the maintenance of body temperature [3], and it can be activated by β -adrenergic activators such as catecholamines [4–7]. Several studies have demonstrated that pheochromocytoma/paraganglioma-secreted catecholamines and BAT can be activated by elevated plasma catecholamines [4,5].

We present the case of a young woman diagnosed with a malignant paraganglioma behind the urinary bladder. FDG-PET/CT showed increased FDG uptake in BAT throughout her body. She also underwent contrast-enhanced CT, which revealed an intense enhancement of contrast medium not only in the primary tumor but also in BAT located at the retroperitoneum and mesentery. We provide characteristic FDG-PET and contrast-enhanced CT image findings of the BAT activated by the patient's pelvic paraganglioma, and we discuss the potential

mechanisms underlying these findings in reference to several relevant reports.

2. Case report

A 17-year-old woman was referred to our hospital after reporting a headache that had persisted for 6 years. She had also suffered from hyperhidrosis, palpitation, and paroxysmal hypertension just after micturition for the prior 3 years. Her systolic blood pressure had occasionally been > 160 mmHg. These symptoms had worsened over the month prior to her referral to us, and she was admitted to our hospital because of a hypertension attack. On admission, she was 153 cm tall and weighed 44.9 kg, with a BMI of 19.2. She had hypertension (200/138 mmHg) and tachycardia (120 beats per min). She has no family or personal history of any malignant or benign neoplasm.

Her serum noradrenaline was 6218 pg/mL (normal \leq 100 pg/mL); her adrenaline level was 54 pg/mL (normal \leq 450 pg/mL), and the dopamine level was 42 pg/mL (normal \leq 20 pg/mL). Her urinary fractionated normetanephrine level was 6.45 μ g/mg·Cre. A 24-hr urine collection test revealed a urinary fractionated normetanephrine level of 4.99 mg/day (normal 0.09–0.33 mg/day) and a noradrenaline level of 2188.8 μ g/day (normal 48.6–168.4 μ g/day). Her HbA1c (NGSP) was 5.7%. The fasting blood glucose level was 143 mg/dL. No gross or microscopic hematuria was detected.

* Corresponding author at: Department of Diagnostic Imaging and Nuclear Medicine, Tokyo Women's Medical University, 8-1, Kawada-cho, Shinjuku-ku, Tokyo 162-8666, Japan.

E-mail address: abe.koichiro@twmu.ac.jp (K. Abe).

<https://doi.org/10.1016/j.ejro.2018.08.002>

Received 21 July 2018; Accepted 12 August 2018

Available online 22 August 2018

2352-0477/© 2018 The Authors. Published by Elsevier Ltd. This is an open access article under the CC BY-NC-ND license (<http://creativecommons.org/licenses/by-nc-nd/4.0/>).

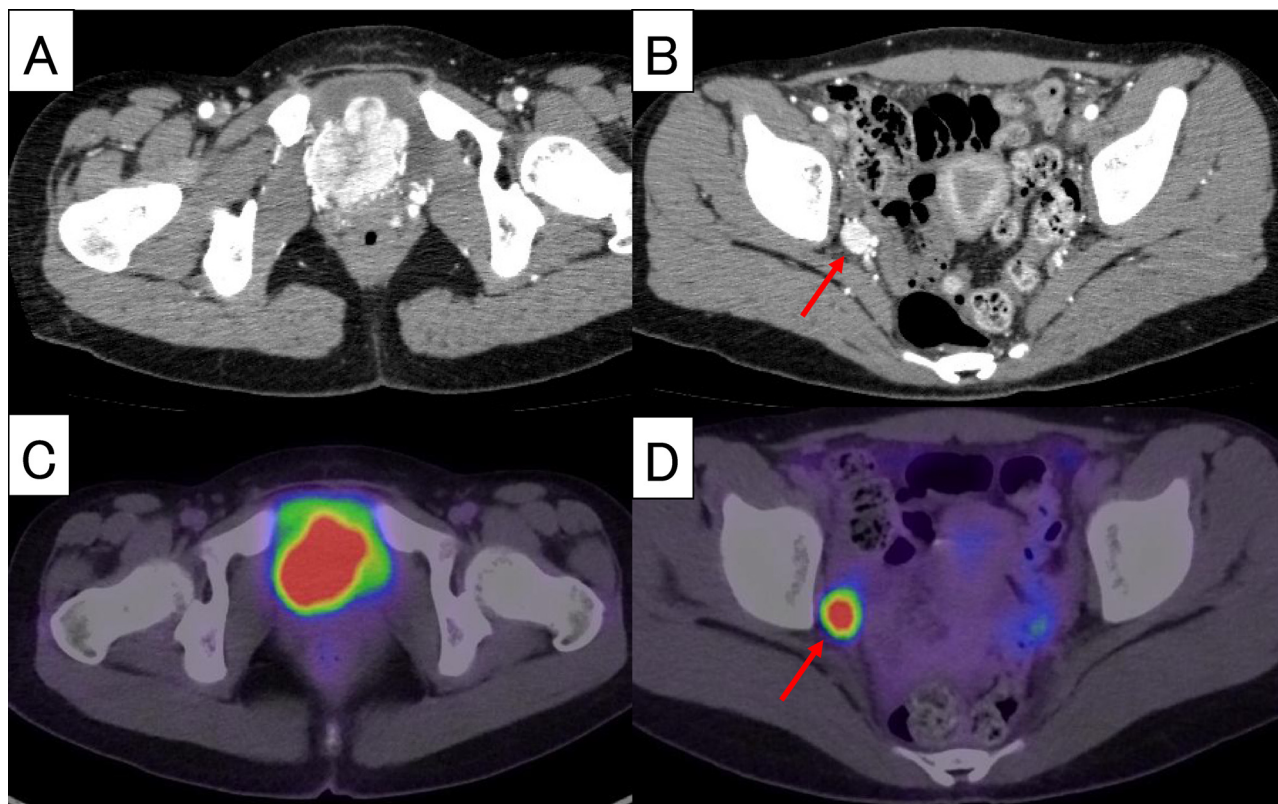


Fig. 1. CT and FDG-PET/CT images of the pelvic paraganglioma and lymph node metastasis of the patient, a 17-year-old female. Axial CT images showed a hypervascular well-defined and lobulated mass (55 mm in long dia.) located dorsocaudal to the urinary bladder (A) and enhanced lymph node swelling (15 mm in short dia.) at the right internal obturator region (B, red arrow). C,D: Intensely high FDG accumulation in the tumor and the lymph node with SUVmax values of 24.7 and 20.8, respectively.

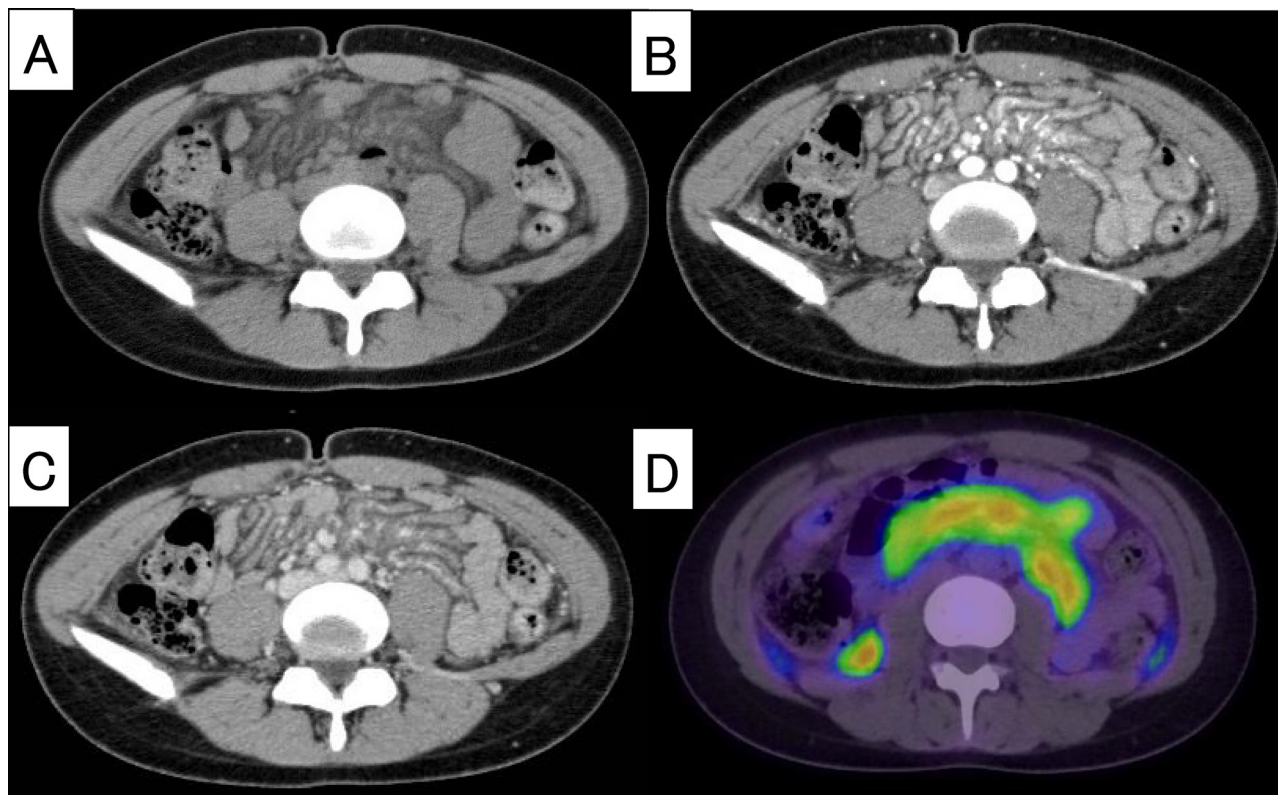


Fig. 2. CT and FDG-PET/CT images of activated mesenteric BAT. A: Axial non-contrast-enhanced CT showed increased attenuation of the visceral fat tissues. Contrast-enhanced CT showed early enhanced (B) and delayed washed out (C) and a spaghetti-like appearance in the mesentery. Intense FDG accumulation in the mesentery was observed (D, SUVmax = 8.1).

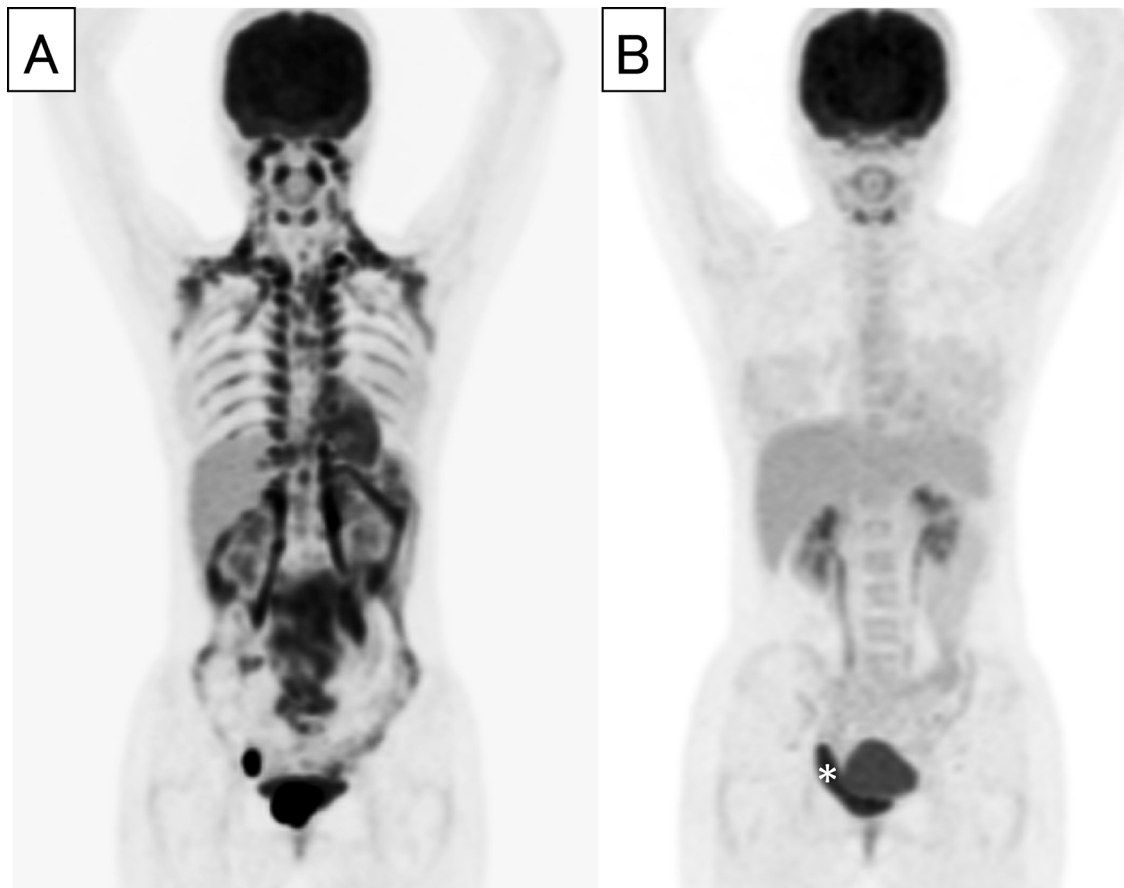


Fig. 3. Pre- and post-surgery FDG-PET MIP images. **A:** Pre-surgery MIP images showed FDG accumulation of BAT in almost the entire body. **B:** Almost all of the FDG accumulations except for a urinary extravasation (*) had disappeared after the surgery.

Abdominal ultrasonography showed an iso- or heterogeneously hyper-echoic tumor behind the urinary bladder, which had abundant blood flow shown by Doppler echo technique. After we brought the patient's blood pressure under control by administering an α 1-blocker, she underwent contrast-enhanced CT. Axial CT images showed a hypervascular well-defined and lobulated mass (55 mm in long dia.) located dorsocaudal to the urinary bladder (Fig. 1A) and intensely enhanced lymph node swelling (15 mm in short dia.) at the right internal obturator region (Fig. 1B). In addition to these lesions, non-contrast-enhanced CT showed increased attenuation of the visceral fat tissues in the parahepatic, paranephric, periadrenal, and mesenteric areas. Contrast-enhanced CT showed thickened mesentery with dilated mesenteric vasculatures, with a “spaghetti-like” appearance (Fig. 2A–C).

Intense FDG uptake was observed in the tumor and right internal obturator lymph node with maximum standardized uptake (SUVmax) values of 24.7 and 20.8, respectively (Fig. 1C, D). Moreover, a whole-body maximum intensity projection (MIP) image showed FDG accumulation in almost the entire body adipose tissue, including the lateral neck, supraclavicular, shoulders, axillary, mediastinum, intercostal paravertebral area, parahepatic area, retroperitoneum including paranephric and periadrenal areas, and mesentery (Fig. 3A). The FDG uptake in the mesenteric fat was so high (SUVmax = 8.1) that the possibility of tumor dissemination could not be denied (Figs. 2D, 3A).

Scintigraphy with I-123 metaiodobenzylguanidine (MIBG) was also performed before the α 1 blocker medication. No significant uptake was seen in the mass, right internal obturator lymph node, or any adipose tissues (data not shown).

We performed a surgical resection of the tumor and right internal obturator lymph node. A brownish and oval tumor was located behind the urinary bladder (Fig. 4A). Hematoxylin-eosin staining showed

atypical cells with stippled chromatin arranged in cell nests (Fig. 4B). Extracapsular and lymphatic invasion was detected. Both chromogranin (Fig. 4C) and synaptophysin (Fig. 4D) immunohistochemistry stains were positive. The Ki-67 proliferative index was 10%–20%. Metastatic foci were also found in the right internal obturator lymph node. Based on these pathological findings, malignant paraganglioma and metastatic lymphadenitis were diagnosed.

After the surgery, all of the patient's symptoms disappeared, and her urinary fractionated metanephrine level decreased to 90.4 μ g/L from 3765.7 μ g/L. A post-surgery FDG-PET/CT examination indicated no abnormal FDG uptake but a little amount of urinary extravasation at the right side of the bladder (Fig. 4B).

3. Discussion

Pheochromocytoma of an adrenal gland and paraganglioma of an extra-adrenal gland are both neuroendocrine tumor (NETs) composed of chromaffin cells. A paraganglioma can develop at the sympathetic trunk around the urinary bladder. As a NET contains catecholamines, mechanical stimulation from the urinary bladder would induce the secretion of catecholamines by an adjacent tumor, followed by a fluctuation of the systemic blood pressure. Our patient had a paraganglioma close to the urinary bladder, and she had experienced hypertension attacks after micturition over a long period of time.

Several imaging modalities are used for the diagnosis of NET. CT is a commonly used imaging tool for detecting tumors (such as paragangliomas) arising from extra-adrenal regions. Although a risk of hypertensive attack after the administration of ionic contrast media in patients with a pheochromocytoma/paraganglioma has been described [8], an intravenous injection of non-ionic contrast media is considered

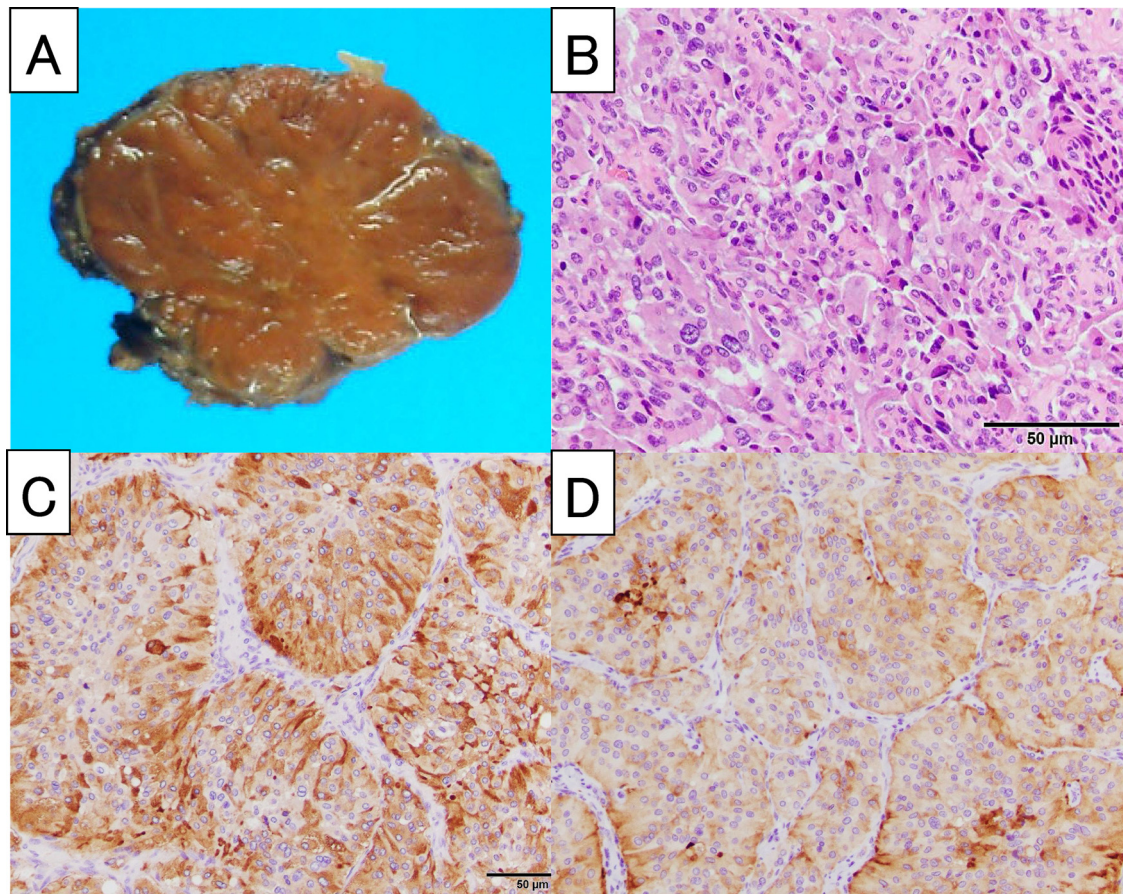


Fig. 4. Pathology of the pelvic paraganglioma. Macroscopic (A) and microscopic features of the pelvic paraganglioma are shown. H&E staining showed atypical cells with stippled chromatin arranged in cell nests (B). Immunohistochemistry showed positivity for chromogranin (C) and synaptophysin (D).

to be relatively safe [9] and useful for the diagnosis. In the present case, we performed CT scanning using non-ionic contrast media after pre-treatment with an α -blocker, and it resulted in no change of the patient's systemic blood pressure. The tumor exhibited an early intense heterogeneous enhancement and washout pattern which was compatible with a NET. Early intense enhancement reflects the capillary-rich framework of paragangliomas [10].

Pheochromocytomas/paragangliomas typically accumulate I-123 MIBG [11], though in our patient's case the I-123 MIBG scintigraphy result was negative. Her serum catecholamine level was so high that MIBG accumulation might have been competitively inhibited. It was reported that most MIBG-negative pheochromocytomas/paragangliomas secreted norepinephrine, not adrenaline [12,13], which is compatible with our patient's case. MIBG negativity was also reported to be associated with its malignant character and SDHB mutation [12,13].

FDG accumulation in paragangliomas was reported with a mean SUVmax of 8.2, though there was no significant difference in the SUVmax between benign and malignant lesions [14]. In the present case, the SUVmax values of both the primary tumor and the lymph node metastasis were extremely high. Another study, tumors with an intense accumulation of FDG tended to have SDH mutation [14]. A genetic analysis of SDHB mutation was not performed in the present case.

In the 1960s, researchers incidentally observed the coexistence of BAT with pheochromocytomas/paragangliomas in resected samples or autopsy specimens [15]. Since the development of FDG-PET, BAT has been easily visualized and was reported to be detected in 19.2%–42% of patients with a pheochromocytoma or paraganglioma [4–7], which is higher than patients without these lesions [2]. Today, it is well known that the activation of BAT is regulated via the sympathetic nervous signals of decreasing body temperature [15,16], and BAT can be

activated by serum catecholamine produced by a pheochromocytoma/paraganglioma [4–7].

Baba et al. showed that activated BAT has higher attenuation than non-activated BAT on non-contrast-enhanced CT, and there were less and smaller lipid vacuoles in the former compared to the latter [17]. Prodhomme et al. reported that the mean attenuation of white fat is -99.5 HU, whereas the mean attenuation of BAT is -32.6 HU on non-contrast-enhanced CT [18]. In contrast-enhanced CT, the CT density of activated BAT is increased [18,19] due to the abundant capillary blood vessels. Activated brown fat has more blood flow than non-activated brown fat [20,21].

BAT is typically observed in the central part of the trunk, e.g., inferior neck-shoulder-supraclavicular, mediastinal, paravertebral, posterior intercostal, and retroperitoneal regions [1,2]. However, the FDG uptake in BAT of an atypical site sometimes hampers accurate diagnoses. Intense FDG accumulation in the mesentery was detected in the present case, based on which peritoneal dissemination of the malignant cells could not be denied. On the other hand, contrast-enhanced CT showed a "spaghetti-like appearance" reflecting enlarged blood vessels in the mesentery, which was clearly different from the findings of a so-called 'omental cake.' Although activated BAT was not histologically confirmed in our patient's case, the postoperative FDG-PET/CT revealed the disappearance of FDG accumulation in the mesentery as well as other sites, suggesting that all were FDG accumulations in BAT.

We have presented the case of a patient who showed characteristic FDG-PET and contrast-enhanced CT finding of BAT activated by a pelvic paraganglioma. Because it might be difficult to discriminate FDG accumulation in the mesenteric BAT from peritoneal dissemination by only FDG-PET/CT, contrast-enhanced CT findings could be helpful to reach the correct diagnosis.

Conflict of interest

The authors declare that they do not have any conflict of interest and did not receive any funding for this work.

Acknowledgments

The authors declare that they do not have any conflict of interest and did not receive any funding for this work.

References

- [1] J.M. Heaton, The distribution of brown adipose tissue in the human, *J. Anat.* 112 (1972) 35–39.
- [2] A.M. Cypess, S. Lehman, G. Williams, I. Tal, D. Rodman, A.B. Goldfine, F.C. Kuo, E.L. Palmer, Y.H. Tseng, A. Doria, G.M. Kolodny, C.R. Kahn, Identification and importance of brown adipose tissue in adult humans, *N. Engl. J. Med.* 360 (2009) 1509–1517.
- [3] F.W. Kiefer, Browning and thermogenic programming of adipose tissue, *Best Pract. Res. Clin. Endocrinol. Metab.* 30 (2016) 479–485.
- [4] M. Hadi, C.C. Chen, M. Whatley, K. Pacak, J.A. Carrasquillo, Brown fat imaging with (18)F-6-fluorodopamine PET/CT, (18)F-FDG PET/CT, and (123)I-MIBG SPECT: a study of patients being evaluated for pheochromocytoma, *J. Nucl. Med.* 48 (2007) 1077–1083.
- [5] Q. Wang, M. Zhang, G. Ning, W. Gu, T. Su, M. Xu, B. Li, W. Wang, Brown adipose tissue in humans is activated by elevated plasma catecholamines levels and is inversely related to central obesity, *PLoS One* 6 (2011) e21006.
- [6] T. Puar, A. van Berkel, M. Gotthardt, B. Havekes, A.R. Hermus, J.W. Lenders, W.D. van Marken Lichtenbelt, Y. Xu, B. Brans, H.J. Timmers, Genotype-dependent brown adipose tissue activation in patients with pheochromocytoma and paraganglioma, *J. Clin. Endocrinol. Metab.* 101 (2016) 224–232.
- [7] C.A. Chang, D.A. Pattison, R.W. Tothill, G. Kong, T.J. Akhurst, R.J. Hicks, M.S. Hofman, (68)Ga-DOTATATE and (18)F-FDG PET/CT in paraganglioma and pheochromocytoma: utility, patterns and heterogeneity, *Cancer Imaging* 16 (2016) 22.
- [8] P. Rossi, I.S. Young, W.F. Panke, Techniques, usefulness, and hazards of arteriography of pheochromocytoma. Review of 99 cases, *JAMA* 205 (1968) 547–553.
- [9] European Society of Urogenital Radiology, *ESUR Guidelines on Contrast Agents v10.0*. (2018) Accessed: June 5, 2018 <http://www.esur-cm.org/index.php/en/>.
- [10] B.K. Park, C.K. Kim, G.Y. Kwon, J.H. Kim, Re-evaluation of pheochromocytomas on delayed contrast-enhanced CT: washout enhancement and other imaging features, *Eur. Radiol.* 17 (2007) 2804–2809.
- [11] V. Rufini, G. Treglia, G. Perotti, A. Giordano, The evolution in the use of MIBG scintigraphy in pheochromocytomas and paragangliomas, *Hormones* 12 (2013) 58–68.
- [12] A. Kurisaki, T. Saito, M. Takahashi, K. Mitani, T. Yao, A case of 123I-MIBG scintigram-negative functioning pheochromocytoma: immunohistochemical and molecular analysis with review of literature, *Int. J. Clin. Exp. Pathol.* 7 (2014) 4438–4447.
- [13] J.S. Fonte, J.F. Robles, C.C. Chen, J. Reynolds, M. Whatley, A. Ling, L.B. Mercado-Asis, K.T. Adams, V. Martucci, T. Fojo, K. Pacak, False-negative ¹²³I-MIBG SPECT is most commonly found in SDHB-related pheochromocytoma or paraganglioma with high frequency to develop metastatic disease, *Endocr. Relat. Cancer* 19 (2012) 83–93.
- [14] D. Taieb, F. Sebag, A. Barlier, L. Tessonier, F.F. Palazzo, I. Morange, P. Niccoli-Sire, N. Fakhry, C. De Micco, S. Cammilleri, A. Enjalbert, J.F. Henry, O. Mundler, 18F-FDG avidity of pheochromocytomas and paragangliomas: A new molecular imaging signature? *J. Nucl. Med.* 50 (2009) 711–717.
- [15] G. Rona, Changes in adipose tissue accompanying pheochromocytoma, *Can. Med. Assoc. J.* 8 (1964) 303–305.
- [16] S. Baba, J.M. Engles, D.L. Huso, T. Ishimori, R.L. Wahl, Comparison of uptake of multiple clinical radiotracers into brown adipose tissue under cold-stimulated and nonstimulated conditions, *J. Nucl. Med.* 48 (2007) 1715–1723.
- [17] S. Baba, H.A. Jacene, J.M. Engles, H. Honda, R.L. Wahl, CT Hounsfield units of brown adipose tissue increase with activation: preclinical and clinical studies, *J. Nucl. Med.* 51 (2010) 246–250.
- [18] H. Prodhomme, J. Ognard, P. Robin, Z. Alavi, P.Y. Salaun, D. Ben Salem, Imaging and identification of brown adipose tissue on CT scan, *Clin. Physiol. Funct. Imaging* 38 (2018) 186–191.
- [19] P. Gupta, P.S. Babyn, A. Shamma, S.F. Miller, Brown fat distribution in the chest wall of infants — normal appearance, distribution and evolution on CT scans of the chest, *Pediatr. Radiol.* 41 (2011) 1020–1027.
- [20] A. Astrup, J. Bülow, J. Madsen, Interscapular brown adipose tissue blood flow in the rat. Determination with ¹³³Xenon clearance compared to the microsphere method, *Pflugers Arch.* 401 (1984) 414–417.
- [21] O. Muzik, T.J. Mangner, W.R. Leonard, A. Kumar, J. Janisse, J.G. Granneman, ¹⁵O PET measurement of blood flow and oxygen consumption in cold-activated human brown fat, *J. Nucl. Med.* 54 (2013) 523–531.